Negative Sequence Current Optimizing Control Based on Railway Static Power Conditioner in V/v Traction Power Supply System

Dinghua Zhang, Zhixue Zhang, *Member, IEEE*, Weian Wang, and Yanling Yang

***Abstract*—In order to bring railway static power conditioner (RPC) into full play in suppressing negative sequence current in the V/v traction power supply system, the reason of negative sequence current and compensation mechanism were analyzed, and the mathematical model with minimum negative sequence current under the constraint of voltage fluctuation, power factor, device capacity, transformer winding capacity, and energy conservation was set up. For solving the small-scale multidimensional nonlinear and constrained optimization problem, an intelligent algorithm based on sequential quadratic programming (SQP) method is proposed through a comparative analysis of existing optimization algorithms and the traditional analytical method. The proposed algorithm is capable to complete an optimizing computation process in several milliseconds with the precision of 0.1 A, and its computational efficiency and precision can meet the needs for real-time control of RPC. A self-adaption real-time optimization computing platform was built in combination with detectable analogue quantities of traction power supply system and RPC, including catenary network voltages, feeder currents, and compensation currents. Simulation and engineering experimentation results are provided to illustrate that the model and its computation are effective and feasible.**

***Index Terms*—Negative sequence current, power quality, railway static power conditioner (RPC), sequential quadratic programming (SQP), V/v traction power supply system.**

I. Introduction

In recent years, China has seen a rapid development in its railway electrification, which is mainly characterized by high speed and heavy load. As the development of power grid relative lags behind the railway, existing old power supply equipments are utilized for most of the traction power supply except passenger dedicated lines. As a result, in such low-capacity power supply systems, power grid is more and more sensitive to the power-quality problems produced with increase of large power locomotive loads. As ac–dc–ac electric locomotives have replaced ac–dc electric locomotives to be the main load [1], the problems of low power factor and low-order harmonics have been relieved. However, with the increase of single-locomotive power and running density in same catenary, big negative sequence current and wide frequency-domain harmonics turn to be the two major problems. The former is particularly acute, motor efficiency of sharing the same power grid is decreased, meanwhile system loss is increased, etc [2]–[7]. Under different topography, scheduling, and working conditions of locomotive, output powers of two-phase windings have significant difference due to imbalance of traction loads, and even one-phase winding provides traction power and the other one absorbs regenerative braking power [8]. If the heavy load locomotive runs on this power supply system, the problem that the single-phase winding cannot provide so big power supply will occur, meanwhile power of the next phase winding will be superfluous. This is caused by improper power distribution in two phases, and the utilization rate of whole transformer is low, meanwhile negative sequence current is high.

To solve such problems, many researches have been carried out in two approaches, i.e., change of power supply mode and addition of compensating device. For the first approach, three-phase power is rectified to dc power and then converted to single-phase ac power for traction network. The traction network and the three-phase power grid is isolated by dc section; therefore, no negative sequence current will be generated under facultative supply mode. In addition, the whole power of traction transformer is circulating [2], [9]–[11], and the phenomenon of insufficient power in the one phase and superfluous power in the next phase will not occur. For the second approach, compensating devices can be added on high-voltage (HV) side of the traction transformer or the traction side [12]–[14]. Static var compensator (SVC) and Static var generator with delta connection can be installed on the HV side, and reactive power and negative sequence current can be suppressed by individual phase control [15]. However, the problem of insufficient power supply caused by improper power distribution of two phases will not be improved in this mode. For compensation on the traction side, negative sequence current is eliminated by controlling power exchange of two-phase windings and producing reactive power independently, and the efficiency of transformer is promoted by active power circulating. Railway static power conditioner (RPC) was initiated by Japanese researchers in 1993, which consists of arbitrary topology ac–dc–ac converter connected to two secondary

Manuscript received September 3, 2014; revised November 12, 2014 and December 29, 2014; accepted February 6, 2015. Date of publication February 20, 2015; date of current version September 21, 2015. Recommended for publication by Associate Editor D. Vinnikov.

D. Zhang and Z. Zhang are with the CSR Research of Electric Technology and Material Engineering, CSR Zhuzhou Electric Locomotive Research Institute Co., Ltd., Hunan 412001, China (e-mail: morose_boy@163.com; zhangzx@csrzic.com).

W. Wang is with the Zhuzhou CSR Times Electric Co., Ltd., CSR Zhuzhou Electric Locomotive Research Institute Co., Ltd., Hunan 412001, China (e-mail: wangwa@163.com).

Y. Yang is with the Department of Information and Electronics, Beijing Institute of Technology, Beijing 100081, China (e-mail: 315144740@qq.com).

Color versions of one or more of the figures in this paper are available online at http://ieeexplore.ieee.org.

Digital Object Identifier 10.1109/TPEL.2015.2404934

windings of traction transformer. The traction power quality can be improved by controlling the quantity of transferred active power, independent reactive power, and harmonics in RPC two ports. Meanwhile, power of traction transformer can be reallocated by controlling transfer of active power between of two windings so that utilization rate of traction transformer is improved, and the problem of insufficient power supply caused by improper power distribution of two phases is solved. These functions of RPC are verified on Japanese Shinkansen in 2002 [16], and becomes a dedicated device against negative sequence current in traction system.

RPC is an effective way for railway authority to have full control over negative sequence current and is also the only means to realize maximum utilization of existing traction transformer. A number of researchers have studied in topologies, control technologies, and capacity calculation methods of RPC [17]–[20]. For example, the 4.2MVA multiple RPC researched by Tsinghua University and Rongxin Power Electronic Co., Ltd., was tested in Nanxiang, Shanghai, in 2009, and the 10MVA cophase power supply system based on RPC is researched by Southwest Jiaotong University, CSR Zhuzhou Electric Locomotive Research Institute Co., Ltd., and other companies, and it was tested in the Meishan Traction Substation of Sichuan in 2011 [21]–[22]. These test results fully verified that RPC possesses the function to realize comprehensive compensations on negative sequence, reactive power, and harmonics, simultaneously. In addition, in order to reduce the capacity of RPC for compensation to reactive power, some researchers have studied and analyzed varied hybrid compensation modes with integrated RPC and LC or SVC [23] to cancel neutral section without electricity; some scholars even have studied cophase power supply based on RPC in combination of catenary rebuilding [21]–[22]. Fruitful results have been achieved in these studies, which laid a solid theoretical and technical foundation for RPC application. In consideration of the device utilization rate and initial investment in actual project, capacity for RPC is designed based on the difference between mean active power of two phase windings as well as the mean reactive power of each phase. Moreover, as large capacity of RPC is restricted by power electronic devices and topology, the capacity of project RPC is generally smaller than needed power. In addition, with rapid increase of railway loads, redundant capacity of RPC is likely to fail to meet the actual requirements in the future. Especially in imbalance traction transformers, RPC not only transfers active power but also provides reactive power to eliminate negative sequence current; it brings about more high capacity than used in balance traction transformers with the same condition. The analytic compensation method was proposed for ensuring both the unity power factor and zero negative sequence current [17], but RPC capacity, voltage fluctuation, and winding capacity are not considered. So, how to obtain the minimum negative sequence current under limited RPC capacity in V/v type or other imbalance transformer is, therefore, an urgent problem of both theoretical and practical significance. Currently, no relevant document is available in this aspect. In this paper, a mathematical model minimizing the absolute value of negative sequent current was established under voltage fluctuation, phase winding capacity, compensation capacity, and other constraints. In order to obtain optimal values of active and reactive power on both ports of RPC, an optimization algorithm based on sequential quadratic sequence was proposed, and the real-time performance and accuracy were analyzed. The engineering prototype system and control strategy of RPC are realized; theoretical analysis is verified by simulation and experiment, simultaneously.

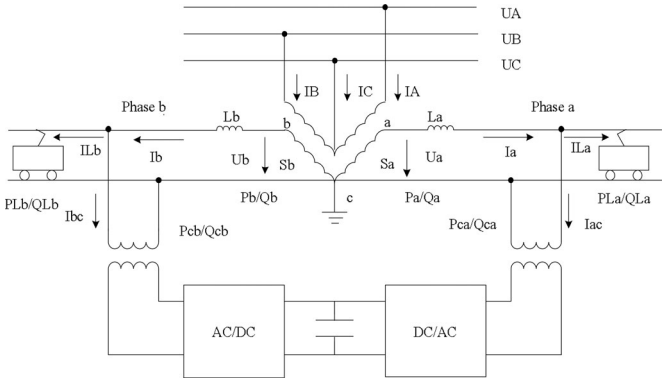

Fig. 1. Schematic diagram of V/V traction power supply system with RPC.

II. Power Optimization Model for RPC-Based V/V Power Supply

A. Expression of Negative Sequence Current

See Fig. 1 for schematic diagram of V/v wired traction power supply system with RPC, and the right feeder section is denoted as Phase a and the left feeder as Phase b. $\dot{I}_{\mathrm{A}}$, $\dot{I}_{\mathrm{B}}$, and $\dot{I}_{\mathrm{C}}$ are three primary phase current of traction transformer, respectively, $\dot{I}_{\mathrm{a}}$ and $\dot{I}_{\mathrm{b}}$ are the feeder current of Phase a and Phase b. θ_{a} is the lagging phase angle of $\dot{I}_{\mathrm{a}}$ against $\dot{U}_{\mathrm{a}}$, and θ_{b} is the lagging phase angle of $\dot{I}_{\mathrm{b}}$ against $\dot{U}_{\mathrm{b}}$. Provided that the turns ratio between primary and secondary winding of traction transformer is k, the negative sequence current $\dot{I}_{\mathrm{a}-}$ and $\dot{I}_{\mathrm{b}-}$ can be obtained with the action of $\dot{I}_{\mathrm{a}}$ and $\dot{I}_{\mathrm{b}}$, respectively, and can be expressed as

$$\dot{I}_{\mathrm{a}-} = \frac{1}{3}(\dot{I}_{\mathrm{A}} + \alpha^2 \dot{I}_{\mathrm{B}} + \alpha \dot{I}_{\mathrm{C}}) = \frac{I_{\mathrm{a}}}{\sqrt{3}k} e^{i(-\frac{\pi}{3}-\theta_{\mathrm{a}})} \quad (1)$$

$$\dot{I}_{\mathrm{b}-} = \frac{1}{3}(\dot{I}_{\mathrm{A}} + \alpha^2 \dot{I}_{\mathrm{B}} + \alpha \dot{I}_{\mathrm{C}}) = \frac{I_{\mathrm{b}}}{\sqrt{3}k} e^{i(\pi-\theta_{\mathrm{a}})}. \quad (2)$$

In the above formula, where $\alpha = e^{i(-\frac{2\pi}{3})}$, all the negative sequence current $\dot{I}_{-}$ can be gained based on the superposition principle

$$\dot{I}_{-} = \dot{I}_{\mathrm{a}-} + \dot{I}_{\mathrm{b}-} = \frac{1}{\sqrt{3}k}(I_{\mathrm{a}} e^{i(-\frac{\pi}{3}-\theta_{\mathrm{a}})} + I_{\mathrm{b}} e^{i(\pi-\theta_{\mathrm{b}})}). \quad (3)$$

Due to Phase a is in-phase with CA phase of three phase, and its negative sequence compensation offset angle is $-\pi/3$, so the compensation angle is the sum of $-\theta_{\mathrm{a}}$ (original power factor angle) and $-\pi/3$. Similarly, due to Phase b is in phase with BC phase of three phase, and its negative sequence compensation

TABLE I
NEGATIVE SEQUENCE CURRENT OFFSET ANGLE OF V/V TRACTION SUBSTATION

Phase in which supply section is connected to the system	Between A and B phases	Between B and C phases	Between C and A phases
Offset angle of negative sequence component	$\pi/3$	π	$-\pi/3$

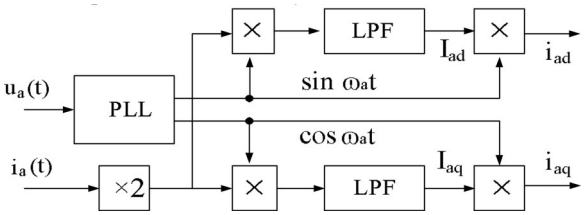

Fig. 2. Vector relation from abc to the *dq* coordinate.

offset angle is π, so the compensation angle is the sum of $-\theta_{\rm a}$ (original power factor angle) and π. Similarly, assume Phase a is in phase with AB phase of three phase, and its negative sequence compensation offset angle is $\pi/3$, so the compensation angle is $-\theta_{\rm a}$ (original power factor angle) plus $\pi/3$, as shown in Table I. Therefore, regardless of the ways of power supply, the total negative sequence component can be obtained by superposition principle.

B. Constraints and the Objective Function

In Fig. 1, it is assumed that the capacity of Phase a supply section is $S_{\rm a}$, and $\dot{I}_{\rm La}$ and $\dot{I}_{\rm ac}$ are the load current and compensating current, respectively. $P_{\rm ca}$ and $Q_{\rm ca}$ are the active power and reactive power of RPC, $P_{\rm a}$ and $Q_{\rm a}$ are the active power and reactive power of feeder, and $P_{\rm La}$ and $Q_{\rm La}$ are the active power and reactive power of load in Phase a, respectively. It is also assumed that the capacity of Phase b supply section is $S_{\rm b}$, and $\dot{I}_{\rm Lb}$ and $\dot{I}_{\rm bc}$ are the load current and compensating current, respectively. $P_{\rm cb}$ and $Q_{\rm cb}$ are the active power and reactive power of RPC, $P_{\rm b}$ and $Q_{\rm b}$ are the active power and reactive power of feeder, and $P_{\rm Lb}$ and $Q_{\rm Lb}$ are the active power and reactive power of load in Phase b, respectively. The transfer principle is shown in Fig. 2, and $U_{\rm ad}$, $U_{\rm aq}$, $\sin\omega_{\rm a}{\rm t}$, and $\cos\omega_{\rm a}{\rm t}$ can be obtained by the phase-locked loop (PLL) for $\dot{U}_{\rm a}$. $\dot{I}_{\rm a}$, and $\dot{I}_{\rm ac}$ can be divided into $I_{\rm ad}$, $I_{\rm aq}$, $I_{\rm acd}$, and $I_{\rm acq}$. Similarly, load current $\dot{I}_{\rm La}$ can be divided into $I_{\rm Lad}$ and $I_{\rm Laq}$.Other variables are decomposed in the same way.

As dc value is more convenient for realizing static error-free tracking control under two-phase *dq* coordinates, active power $P_{\rm a}$ and reactive power $Q_{\rm a}$ of Phase a winding, and active power $P_{\rm ca}$ and reactive power $Q_{\rm ca}$ of Phase a port of RPC are expressed using $U_{\rm ad}$, $I_{\rm ad}$, $I_{\rm aq}$, $I_{\rm acd}$, and $I_{\rm acq}$, in the following formula:

$$\begin{cases} P_{\rm a} = \frac{1}{2} U_{\rm ad} \bullet I_{\rm ad} \\ Q_{\rm a} = \frac{1}{2} U_{\rm ad} \bullet I_{\rm aq} \end{cases} \tag{4}$$

$$\begin{cases} P_{\rm ca} = \frac{1}{2} U_{\rm ad} \bullet I_{\rm acd} \\ Q_{\rm ca} = \frac{1}{2} U_{\rm ad} \bullet I_{\rm acq} \end{cases}. \tag{5}$$

Similarly, through phase locking of $\dot{U}_{\rm b}$, $U_{\rm bd}$, $U_{\rm bq}$, $\sin\omega_{\rm b}{\rm t}$, and $\cos\omega_{\rm b}{\rm t}$ can be obtained. $\dot{I}_{\rm b}$ and $\dot{I}_{\rm bc}$ can be divided into $I_{\rm bd}$, $I_{\rm bq}$ and $I_{\rm bcd}$, $I_{\rm bcq}$ by trigonometric function value of $\sin\omega_{\rm b}t$ and $\cos\omega_{\rm b}t$. Load current $\dot{I}_{\rm Lb}$ can be divided into $I_{\rm Lbd}$ and $I_{\rm Lbq}$. Active power $P_{\rm b}$ and reactive power $Q_{\rm b}$ of Phase b of traction power supply and active power $P_{\rm cb}$ and reactive power $Q_{\rm cb}$ of the Phase b port of RPC are expressed with $U_{\rm bd}$, $I_{\rm bd}$, $I_{\rm bq}$, $I_{\rm bcd}$, and $I_{\rm bcq}$, in the following formula:

$$\begin{cases} P_{\rm b} = \frac{1}{2} U_{\rm bd} \bullet I_{\rm bd} \\ Q_{\rm b} = \frac{1}{2} U_{\rm bd} \bullet I_{\rm bq} \end{cases} \tag{6}$$

$$\begin{cases} P_{\rm cb} = \frac{1}{2} U_{\rm bd} \bullet I_{\rm bcd} \\ Q_{\rm cb} = \frac{1}{2} U_{\rm bd} \bullet I_{\rm bcq} \end{cases}. \tag{7}$$

1) Restriction of Voltage Fluctuation Range: The impedance is high for both of small traction transformer and traction network line, and the fluctuation of electric locomotive load is high too. So the voltage of traction network changes drastically, and both overvoltage and undervoltage impose unfavorable impact on electric locomotives: Overvoltage will damage the electric insulation of the locomotive, while undervoltage will result in insufficient traction of the locomotive and consequent reduction in velocity. For important auxiliary machines including air compressor, traction motor, and ventilator particularly, low voltage is likely to cause insufficient torque, which can result in such safety hazards as inadequate air braking force and overheating of traction motor. Assume ΔU_1 is the voltage drop, which is produced by reactive current in inductive reactance, and ΔU_2 is the voltage drop, which is produced by active current in resistance. ΔU_1 and ΔU_2 have the same phase with the ideal voltage of the electric traction network. Meanwhile, assume ΔU_3 is defined as the voltage drop of reactive current in resistance, and ΔU_4 is the voltage drop of active current in inductive reactance. ΔU_3 and ΔU_4 are perpendicular to the ideal voltage of the electric traction network. Voltage drop in the horizontal direction contributes much more to the fluctuation in traction network voltage than that in the perpendicular direction; and as such ΔU_1 and ΔU_2 are the primary cause for voltage fluctuation, and ΔU_3 and ΔU_4 are negligible for the purpose of this discussion. In Fig. 1, it is assumed that $L_{\rm a}$ and $R_{\rm a}$, and $L_{\rm b}$ and $R_{\rm b}$ are the impedance and resistance of Phase a and Phase b, respectively, and the total voltage drop of Phase a winding $\Delta U_{\rm a}$ and the total voltage drop of Phase b winding $\Delta U_{\rm b}$ are following:

$$\begin{cases} \Delta U_{\rm a} = \frac{1}{\sqrt{2}} (I_{\rm aq} \bullet \omega L_{\rm a} + I_{\rm ad} \bullet R_{\rm a}) \\ \Delta U_{\rm b} = \frac{1}{\sqrt{2}} (I_{\rm bq} \bullet \omega L_{\rm b} + I_{\rm bd} \bullet R_{\rm b}) \end{cases} \tag{8}$$

where I_{aq} and I_{bq}, and I_{ad} and I_{bd} are reactive current component and active current component of winding current I_{a} and I_{b} respectively. Let us further assume the maximum and minimum value of the fluctuated voltage as $U_{\max+}$ and $U_{\max-}$, respectively, then they shall meet the following requirements:

$$\begin{cases} \sqrt{2}U_{\max-} \le I_{\mathrm{aq}} \bullet \omega L_{\mathrm{a}} + I_{\mathrm{ad}} \bullet R_{\mathrm{a}} \le \sqrt{2}U_{\max+} \\ \sqrt{2}U_{\max-} \le I_{\mathrm{bq}} \bullet \omega L_{\mathrm{b}} + I_{\mathrm{bd}} \bullet R_{\mathrm{b}} \le \sqrt{2}U_{\max+} \end{cases}. \tag{9}$$

2) Restriction of Total Power Factor: Although the check point of power factor is the three-phase entrance of transformer, the reactive power loss due to the leakage reactance of the transformer is relatively less. As long as the reactive power on the traction side after compensation satisfies formula (10), the requirement that the power factor of the electric traction system shall not be less than k_{f} can be met, and monetary penalty due to insufficient power factor can be avoided. Formula (10) can also be written in its equivalent form, formula (11) using U_{ad}, U_{bd}, I_{ad}, I_{bd}, I_{aq}, and I_{bq} as follows:

$$P_{\mathrm{a}} + P_{\mathrm{b}} \ge k_{\mathrm{f}} \sqrt{(P_{\mathrm{a}} + P_{\mathrm{b}})^2 + (Q_{\mathrm{a}} + Q_{\mathrm{b}})^2} \tag{10}$$

$$\begin{aligned} &U_{\mathrm{ad}} \bullet I_{\mathrm{ad}} + U_{\mathrm{bd}} \bullet I_{\mathrm{bd}} \\ &\ge k_{\mathrm{f}} \sqrt{\begin{array}{l} (U_{\mathrm{ad}} \bullet I_{\mathrm{ad}} + U_{\mathrm{bd}} \bullet I_{\mathrm{bd}})^2 \\ +(U_{\mathrm{ad}} \bullet I_{\mathrm{aq}} + U_{\mathrm{bd}} \bullet I_{\mathrm{bq}})^2 \end{array}}. \end{aligned} \tag{11}$$

3) Restriction of Equipment Capacity: As the total current is limited by power electronic device, the instantaneous value of I_{ac} and I_{bc} of RPC are restricted in any condition. Assumed the maximum of device is $I_{\mathrm{c\,max}}$, the rule that I_{ac} and I_{bc} are less than I_{bc} must be satisfied. Restricted by equipment on the dc side of the RPC, the maximum of transferred active power is $P_{\max}$. In order to realize heat dissipation and stability, the actual transferred active power P_{c} is not greater than $P_{\max}$

$$\begin{cases} |P_{\mathrm{c}}| \le (P_{\max}) \\ |I_{\mathrm{ac}}| \le I_{\mathrm{cmax}} \\ |I_{\mathrm{bc}}| \le I_{\mathrm{cmax}} \end{cases}. \tag{12}$$

It can be expressed by voltage and current as

$$\begin{cases} |\frac{1}{2}U_{\mathrm{ad}} \bullet I_{\mathrm{acd}}| \le (P_{\max}) \\ |\frac{1}{2}U_{\mathrm{bd}} \bullet I_{\mathrm{bcd}}| \le (P_{\max}) \\ \sqrt{I_{\mathrm{acd}}^2 + I_{\mathrm{acq}}^2} \le I_{\mathrm{c\,max}} \\ \sqrt{I_{\mathrm{bcd}}^2 + I_{\mathrm{bcq}}^2} \le I_{\mathrm{c\,max}} \end{cases}. \tag{13}$$

4) Restriction of Transformer Capacity: As the capacity of the transformer is limited, the instantaneous power of Phase a and Phase b after compensation shall not be greater than the rated capacity of each winding, i.e. S_{a} and S_{b}. That is, they shall meet given formula

$$\begin{cases} \sqrt{P_{\mathrm{a}}^2 + Q_a^2} \le S_{\mathrm{a}} \\ \sqrt{P_{\mathrm{b}}^2 + Q_{\mathrm{b}}^2} \le S_{\mathrm{b}} \end{cases}. \tag{14}$$

It can be expressed by voltage and current as

$$\begin{cases} \frac{1}{2}U_{\mathrm{ad}} \bullet \sqrt{I_{\mathrm{ad}}^2 + I_{\mathrm{aq}}^2} \le S_{\mathrm{a}} \\ \frac{1}{2}U_{\mathrm{bd}} \bullet \sqrt{I_{\mathrm{bd}}^2 + I_{\mathrm{bq}}^2} \le S_{\mathrm{b}} \end{cases}. \tag{15}$$

5) Restriction of Equal Active Power Transmitted: As the loss of RPC is neglected, and compensating device does not produce active power, the active powers transmitted by both ports of RPC, therefore, are equal

$$U_{\mathrm{ad}} \bullet I_{\mathrm{acd}} = -U_{\mathrm{bd}} \bullet I_{\mathrm{bcd}}. \tag{16}$$

6) Objective Function: The module value is the minimum when the objective function is a negative sequence current vector. It is expanded from the Euler's formula $e^{i\theta} = \cos\theta + i\sin\theta$ by combining with formula (3)

$$\begin{aligned} \min|\dot{I}_-| &= \min\left|\frac{1}{\sqrt{3}k}\left(I_{\mathrm{a}}e^{i(-\frac{\pi}{3}-\theta_{\mathrm{a}})} + I_b e^{i(\pi-\theta_{\mathrm{b}})}\right)\right| \\ &= \frac{1}{\sqrt{3}k}\min\sqrt{\begin{array}{l} \left[\sqrt{I_{\mathrm{ad}}^2 + I_{\mathrm{aq}}^2}\left(\frac{\cos\theta_{\mathrm{a}}}{2} - \frac{\sqrt{3}\sin\theta_{\mathrm{a}}}{2}\right)\right. \\ \left. -\sqrt{I_{\mathrm{bd}}^2 + I_{\mathrm{bq}}^2}\cos(\theta_{\mathrm{b}})\right]^2 \\ +\left[\sqrt{I_{\mathrm{ad}}^2 + I_{\mathrm{aq}}^2}\left(-\frac{\sqrt{3}\cos\theta_{\mathrm{a}}}{2} - \frac{1\sin\theta_{\mathrm{a}}}{2}\right)\right. \\ \left. +\sqrt{I_{\mathrm{bd}}^2 + I_{\mathrm{bq}}^2}\sin(\theta_{\mathrm{b}})\right]^2 \end{array}} \end{aligned} \tag{17}$$

where $\theta_{\mathrm{a}} = \arctan(I_{\mathrm{aq}}/I_{\mathrm{ad}})$ and $\theta_b = \arctan(I_{bq}/I_{bd})$. In the mathematical model established by the above constraint condition and objective functions, L_{a}, R_{a}, L_{b}, R_{b}, $U_{\max-}$, $U_{\max+}$, k_{f}, $P_{\max}$, $I_{\mathrm{c\,max}}$, S_{a}, and S_{b} are determined by the actual parameter and demand of the electric traction network, U_{ad} and U_{bd} are determined by real-time feedback value by the winding voltage of Phase a and Phase b of the traction transformer, which can also be regarded as known values. Therefore, only variables I_{acd}, I_{acq}, I_{bcd}, and I_{bcq} are unknown and need to be solved. It can be seen from KCL theorem that I_{ad} and I_{aq} are collectively determined by I_{acd} and I_{acq} and actual load I_{Lad} and I_{Laq}. That is, they shall satisfy

$$\begin{cases} I_{\mathrm{ad}} = I_{\mathrm{Lad}} + I_{\mathrm{acd}} \\ I_{\mathrm{aq}} = I_{\mathrm{Laq}} + I_{\mathrm{acq}} \end{cases}. \tag{18}$$

Similarly, we also have formula (19).

$$\begin{cases} I_{\mathrm{bd}} = I_{\mathrm{Lbd}} + I_{\mathrm{bcd}} \\ I_{\mathrm{bq}} = I_{\mathrm{Lbq}} + I_{\mathrm{bcq}} \end{cases} \tag{19}$$

In the above two formulas, I_{Lad}, I_{Laq}, I_{Lbd}, and I_{Lbq} are determined by the actual load and can be regarded as known values. Therefore, I_{acd}, I_{acq}, I_{bcd}, and I_{bcq} need to be found in this mathematical model for a satisfactory solution.

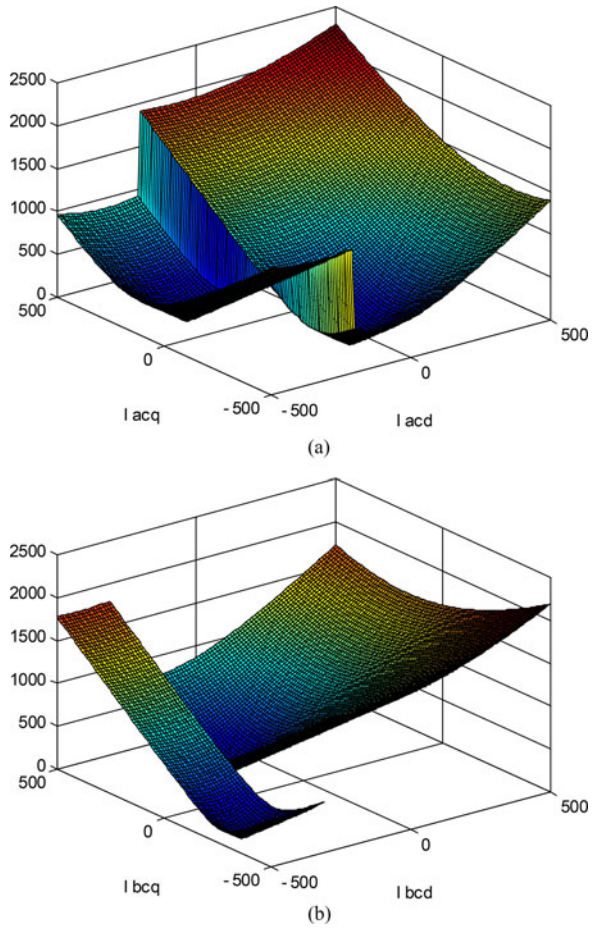

Fig. 3. Nonlinear objective function of the negative sequence current optimization problem (local). (a) Optimizing path of variables in Phase a. (b) Optimizing path of variables in Phase b.

III. Negative Sequence Current Optimal Computation

A. Feature analysis of optimization objective

In essence, optimization of negative sequence current is a single objective solution problem about multidimensional strong coupling and multinonlinear constrained optimization. There are three factors for the optimization problem, namely, decision vector, objective function, and constraint conditions. The decision vector of negative sequence current optimization is $\left[I_{\mathrm{acd}}\ I_{\mathrm{acq}}\ I_{\mathrm{bcd}}\ I_{\mathrm{bcq}} \right]^{\mathrm{T}}$, a four-dimensional decision vector, and the objective function is the minimum value of $|\dot{I}_{-}|$. Constraints include both inequality and equality constraints.

Strong nonlinear characteristics of function are shown in Fig. 3, and simulation parameters are in consistent with Table II. The optimizing process of objective function $|\dot{I}_{-}|$ varying with I_{acd} and I_{acq} within the range of $[-500, 500]$ when $I_{\mathrm{bcd}} = I_{\mathrm{bcq}} = -50$ is shown in Fig. 3(a) and (b) shows the optimizing process of the objective function $|\dot{I}_{-}|$ varying with I_{bcd} and I_{bcq} within the range of $[-500, 500]$ when $I_{\mathrm{acd}} = I_{\mathrm{acq}} = -50$.

It can be seen from Fig. 3 that the optimizing problem not only displays a nonlinear variation trend but also exhibits obvious fault faces geometrically. Thus, this problem is an irregular multidimensional nonlinear constrained optimization problem. Due to the arbitrariness of nonlinear question, it is usually difficult to obtain results by a direct approach. Specialized numerical optimization algorithms such as substitution method, active set theory, interior point approximation, sequential subproblem approximation, and so on are needed. SQP method [24] and modern interior point (MIP) method [25] are typical of these algorithms. As for calculation load, though the load of each iteration of MIP method is larger than that of SQP method, the number of iterations to achieve optimal solution is less than that of SQP method. In comprehensive comparison, the computational efficiency is higher for small- and medium-scale nonlinear constrained optimization problem when SQP method is adopted. As for large-scale problems with thousands of decision variables and constraints, MIP method is superior to SQP method. In particular, the modulus minimization problem of negative sequence current, with only four decision vectors, is a small-scale problem, and therefore, SQP method is more suitable for this purpose than others.

B. Comparison Analysis Between SQP and MIP

In order to test the result from theoretical analysis, we conducted a research on two algorithms under two typical working conditions for their performance, which is characterized by precision, stability, and time consumed. One of the typical working conditions is taken as an example for introduction. In the working condition, the loads of Phase a and Phase b are in the traction condition, and the active current of both are larger than the reactive current. Relative parameters are shown in Table II.

The expression of nonnonlinear constraint optimization problem can be obtained by putting the parameter values above into the expression from (8) to (19). In the expression (20), TermI and TermII are assumed to be the real part and imaginary part of the negative sequence current vector $\dot{I}_{-}$, respectively

$$\min \sqrt{\mathrm{TermI}^2 + \mathrm{TermII}^2}$$
$$\text{s.t.} \begin{cases} I_{\mathrm{acd}} + I_{\mathrm{bcd}} = 0 \\ 96\left(I_{\mathrm{acd}} + I_{\mathrm{bcd}} + 500\right)^2 - 529\left(I_{\mathrm{acq}} + I_{\mathrm{bcq}} + 150\right)^2 \geq 0 \\ 360000 - I_{\mathrm{acd}}^2 - I_{\mathrm{acq}}^2 \geq 0 \\ 360000 - I_{\mathrm{bcd}}^2 - I_{\mathrm{bcq}}^2 \geq 0 \\ 1731301.93905817 - \left(I_{\mathrm{acq}} + 100\right)^2 - \left(I_{\mathrm{acd}} + 200\right)^2 \geq 0 \\ 1731301.93905817 - \left(I_{\mathrm{bcq}} + 50\right)^2 - \left(I_{\mathrm{bcd}} + 300\right)^2 \geq 0 \\ -421.0526316 \leq I_{\mathrm{acd}} \leq 421.0526316 \\ -7071.067812 \leq (I_{\mathrm{acq}} + 100)^{*}1.57 + (I_{\mathrm{acd}} + \\ 200)^{*}0.2 \leq 7071.067812 \\ -421.0526316 \leq I_{\mathrm{bcd}} \leq 421.0526316 \\ -7071.067812 \leq (I_{\mathrm{bcq}} + 50)^{*}1.57 + (I_{\mathrm{bcd}} + \\ 300)^{*}0.2 \leq 7071.067812 \end{cases} \tag{20}$$

TABLE II
PARAMETERS UNDER TYPICAL WORKING CONDITIONS

Description	Parameter symbols	Typical working condition values	Descriptions	Parameter symbols	Typical working condition values
Load active current of Phase a	I_{Lad}	200 (A)	D component of reference voltage of Phase b	U_{bd}	38 000 (V)
Load reactive current of Phase a	I_{Laq}	100 (A)	Negative maximum voltage fluctuation	U_{min}	–5000 (V)
Load active current of Phase b	I_{Lbd}	300 (A)	Positive maximum voltage fluctuation	U_{max}	5000 (V)
Load reactive current of Phase b	I_{Lbq}	50 (A)	Capacity of RPC	P_{max}	8 (MW)
Winding reactance of Phase a	ωL_{a}	1.57 (Ω)	Maximum current of RPC	I_{cmax}	600 (A)
Winding resistance of Phase a	R_{a}	0.2 (Ω)	Power supply capacity of Phase a	S_{a}	25 (MVA)
Winding reactance of Phase b	ωL_{b}	1.57 (Ω)	Power supply capacity of Phase b	S_{b}	25 (MVA)
Winding resistance of Phase b	R_{b}	0.2 (Ω)	Turns ratio of transformer	k	4
D component of reference voltage of Phase a	U_{ad}	38 000 (V)	Target power factor	k_{f}	0.92

Problem (20) is a multidimensional nonlinear constrained optimization problem with four decision variables I_{acd}, I_{acq}, I_{bcd}, and I_{bcq}, including one equality constraint and thirteen inequality constraints. Due to the complexity of the expressions of TermI and TermII in objective junction, they are listed below separately as follows:

$$\mathrm{TermI} = \frac{1}{4\sqrt{3}} \sin\left(-\frac{\pi}{3} - \arctan\left(\frac{I_{\mathrm{acq}}+100}{I_{\mathrm{acd}}+200}\right)\right) \sqrt{\begin{matrix}(I_{\mathrm{acq}+100})^2+\\ (I_{\mathrm{acd}}+200)^2\end{matrix}} + \frac{1}{4\sqrt{3}} \frac{\sqrt{(I_{\mathrm{bcq}}+50)^2+(I_{\mathrm{bcd}}+300)^2}\,(I_{\mathrm{bcq}}+50)}{(I_{\mathrm{bcd}}+300)\sqrt{\frac{(I_{\mathrm{bcq}}+50)^2}{(I_{\mathrm{bcq}}+300)^2}+1}} \tag{21}$$

$$\mathrm{TermII} = \frac{1}{4\sqrt{3}} \frac{\sqrt{(I_{\mathrm{bcq}}+50)^2+(I_{\mathrm{bcd}}+300)^2}}{\sqrt{\frac{(I_{\mathrm{bcq}}+50)^2}{(I_{\mathrm{bcd}}+300)^2}+1}} - \frac{1}{4\sqrt{3}} * \cos\left(-\frac{\pi}{3} - \arctan\left(\frac{I_{\mathrm{acq}}+100}{I_{\mathrm{acd}}+200}\right)\right) \sqrt{(I_{\mathrm{acq}}+100)^2+(I_{\mathrm{acd}}+200)^2}. \tag{22}$$

SQP method is adopted for the solution of problem (20). Initial values are set as $I_{\mathrm{acd}} = 51$, $I_{\mathrm{acq}} = -100$, $I_{\mathrm{bcd}} = -49$, and $I_{\mathrm{bcq}} = -50$, while the precision is set as 10^{-2} and maximal time is set as 5×10^{-2}s. The results obtained are shown in Table III. It can be seen from the table above that the optimal decision variable obtained through SQP method is $(I^*_{\mathrm{acd}}, I^*_{\mathrm{acq}}, I^*_{\mathrm{bcd}}, I^*_{\mathrm{bcq}}) = (50.0, -244.3, -50.0, 94.3)$. The corresponding module value of $|\dot{I}_-|$ is $0.009\,4$ A, which is close to zero, and constraints are satisfied at the same time. The number of estimation and time-consuming are two important factors for evaluating the efficiency of optimization algorithm. To meet the accuracy of 10^{-2}, 30 times of iterations and 2948 times of estimation in total are necessary when SQP method is adopted. It will take about 0.007 s for the calculation on an A10-6700 computing platform with quad-core processor (3.7G/8G memory). And then, interior point method is adopted to solve the problem again with the same initial value and precision. The results are shown in Table III. The minimum module value of negative sequence current obtained by using MIP method is 0.2091A. Although constraint conditions are still satisfied, the results are far less satisfactory than those obtained by using SQP method. 241 times of iterations are needed in the optimizing process, and 364 543 times of estimation in total are used, and the entire process consumes 0.05 s. All these indexes are worse than the SQP method.

In order to compare the stability of the two algorithms, different initial values are randomly selected. The results are shown in Table IV, the minimum module value of negative sequence current $I^*_- = 1.65 \times 10^{-2}$ A was obtained by using SQP method with 34 times of iterations, 3467 times of estimation, and a time consumed of 0.009 s, when the initial value is $(I_{\mathrm{acd}}, I_{\mathrm{acq}}, I_{\mathrm{bcd}}, I_{\mathrm{bcq}}) = (50, 50, -50, -50)$, while 124 times of iteration and 325 416 times of estimation were needed to obtain the minimum module value $I^*_- = 1.55 \times 10^{-2}$ A by using MIP method. But the time consumed in estimating the value of functions is longer being 0.03 s. In terms of efficiency, combined with results obtained under some other working conditions, it can be concluded that the effect of SQP method is better than MIP method.

Combined with the initial parameters in Table II and the optimization results by SQP in Table III, the change of current distribution and negative sequence current before and after compensation were analyzed. Fig. 4(a) illustrates the relation among the three vectors under Phase a: feeder section load current i_{La}, compensation current i_{ac}, and total current i_{a}. It can be seen that the current i_{a} is the vector sum of load current i_{La} and compensation current i_{ac}, and the amplitude of i_{a} has increased after compensation. Suppose voltage vector U_{a} is referenced zero vector, the phase angle of i_{a} has decreased form positive value to negative value after compensation. Similarly, Fig. 4(b) shows

TABLE III
PROBLEM SOLVING BASED ON SQP METHOD AND MIP METHOD

Algorithm	Initial value (A)	Optimal value (A)	Optimal objective function value (A)	Number of iterations	Estimation number of function	Time-consuming (s)
SQP	$I_{\mathrm{acd}}=51$ $I_{\mathrm{acq}}=-100$	$I^*_{\mathrm{acd}}=50.0\, I^*_{\mathrm{acq}}=-244.3$ $I^*_{\mathrm{bcd}}=-50.0\, I^*_{\mathrm{bcq}}=94.3$	$I^*_-=0.0094$	30	2948	0.007
MIP	$I_{\mathrm{bcd}}=-49$ $I_{\mathrm{bcq}}=-50$	$I^*_{\mathrm{acd}}=52.1\, I^*_{\mathrm{acq}}=-240.4$ $I^*_{\mathrm{bcd}}=-52.1\, I^*_{\mathrm{bcq}}=96.7$,,	$I^*_-=0.2091$	241	364 543	0.05

TABLE IV
PROBLEM SOLVING UNDER DIFFERENT INITIAL VALUES

Algorithm	Initial value of $I_{\mathrm{acd}}, I_{\mathrm{acq}}, I_{\mathrm{bcd}}, I_{\mathrm{bcq}}$ (A)	Optimal objective function value (A)	Number of iterations	Estimation number of function	Time consumed (s)
SQP method	$(0,0,0,0)$	$I^*_-=2.25\times10^{-2}$	32	3146	0.008
	$(50,50,-50,-50)$	$I^*_-=1.65\times10^{-2}$	34	3467	0.009
	$(70,-90,-65,-50)$	$I^*_-=1.8\times10^{-2}$	46	6081	0.010
MIP method	$(0,0,0,0)$	$I^*_-=2.29\times10^{-2}$	189	352 147	0.050
	$(50,50,-50,-50)$	$I^*_-=1.55\times10^{-2}$	124	325 416	0.038
	$(70,-90,-65,-50)$	$I^*_-=1.91\times10^{-2}$	156	347 283	0.043

the relation among the three vectors under Phase b: feeder section load current i_{La}, compensation current i_{bc}, and total current i_{b}; it can be seen that the total current i_{b} is the vector sum of load current i_{La} and compensation current i_{bc}, and the amplitude of compensated current i_{b} has decreased. Suppose voltage vector U_{b} is referenced zero vector, the phase angle of i_{b} has increased after compensation. After compensation, the amplitudes of i_{a} and i_{b} are the same. When the angle of vector U_{A} is zero, the phase angle of i_{a} after compensation is zero too, and the phase angle of i_{b} after compensation is $-2\pi/3$, which means the difference between i_{a} and i_{b} is $2\pi/3$. To sum up, the amplitudes of i_{a} and i_{b} are the same, the difference of phase angle value is $2\pi/3$, the negative sequence current generated by them is zero. This can also be verified in Fig. 5. It can be seen from Fig. 5(a) that three-phase current before compensation are$I_{\mathrm{A\text{-}p}}$, $I_{\mathrm{B\text{-}p}}$, $I_{\mathrm{C\text{-}p}}$, and the amplitudes are unequal; and the phase angles are inconsistent with positive sequence distribution. It can be seen from Fig. 5(b) that negative sequence current $I_{\mathrm{\text{-}p}}$ before compensation is approximately is 55A. After compensation, however, the amplitude of I_{A}, I_{B}, and I_{C} are the same, and phase angles tally with positive sequence distribution. Negative sequence current after compensation is I_-, and its value is almost 0 A [see Fig. 5(b)].

C. Comparison Analysis Between SQP and the Analytical Method

According to [17], combined with the definition of variable relationship in this paper, the formula of analysis method can be derived as follows:

$$\begin{cases} I_{\mathrm{acd}} = -\frac{1}{2}(I_{\mathrm{Lad}} - I_{\mathrm{Lbd}}) \\ I_{\mathrm{bcd}} = \frac{1}{2}(I_{\mathrm{Lad}} - I_{\mathrm{Lbd}}) \\ I_{\mathrm{acq}} = -I_{\mathrm{Laq}} - \frac{1}{2\sqrt{3}}(I_{\mathrm{Lad}} + I_{\mathrm{Lbd}}) \\ I_{\mathrm{bcq}} = -I_{\mathrm{Lbq}} + \frac{1}{2\sqrt{3}}(I_{\mathrm{Lad}} + I_{\mathrm{Lbd}}) \end{cases} \tag{23}$$

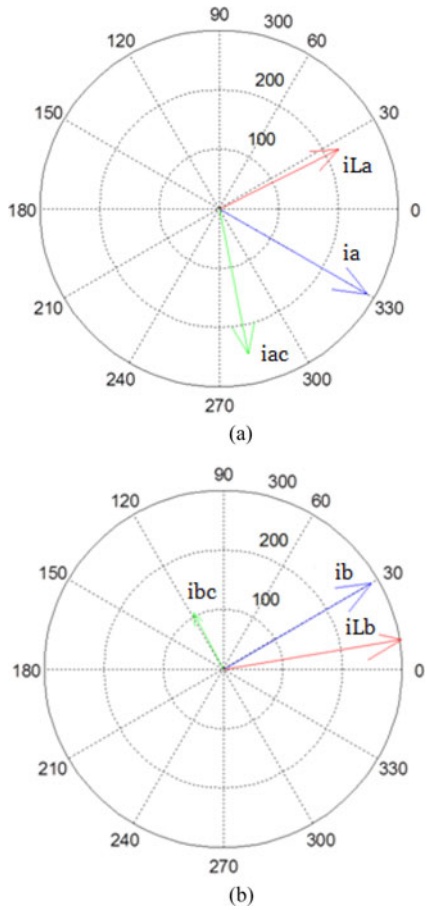

Fig. 4. Distributions of load current, compensation current, and total current of two feeder sections. (a) Vector relation among Phase a currents. (b) Vector relation among Phase b currents.

Combining with the parameters in the Table II, when [I_{Lad} I_{Laq} I_{Lbd} I_{Lbq}] is [200 100 300 50], the value of [I_{acd} I_{acq} I_{bcd} I_{bcq}] is [200 100 300 50] by the formula (23), the results are consistent with SQP method. This is because in this particular case,

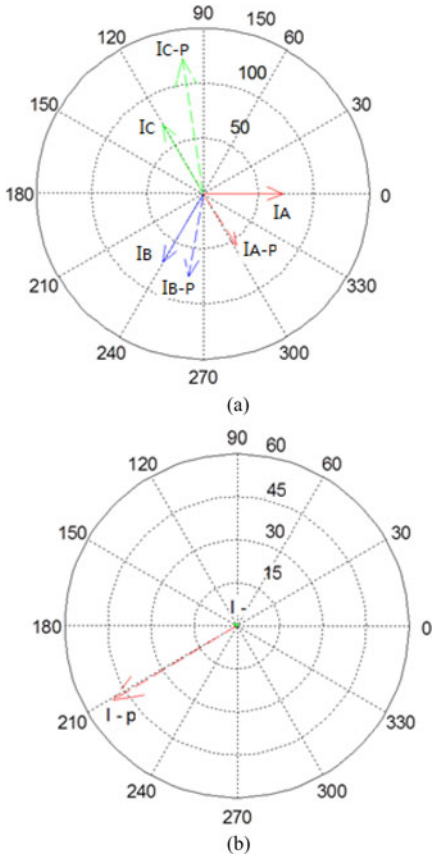

Fig. 5. Three-phase currents and negative sequence current on HV side before and after compensation. (a) Distribution of three-phase currents before and after compensation. (b) Distribution of negative sequence currents before and after compensation.

the results are not limited by any constraint in this model. Assume that when $[I_{\mathrm{Lad}}\ I_{\mathrm{Laq}}\ I_{\mathrm{Lbd}}\ I_{\mathrm{Lbq}}]$ is [700 500 200 100], the optimal value of $[I_{\mathrm{acd}}\ I_{\mathrm{acq}}\ I_{\mathrm{bcd}}\ I_{\mathrm{bcq}}]$ is [−147.7 −581.5 147.7 334.3] by SQP method, but another result is [−250 −759.8 250 159.8] by analytical method. The negative sequence current and constraint values based on the two methods are analyzed in Table V, the negative sequence current is 0.0019 A by analytical method, and the value is 0.4903 A by SQP method, and the precision of each other is higher than 10^{-1} A. But the absolute current of the Phase a port of RPC, namely $|I_{\mathrm{ac}}|$ reaches to 799.87 A, and exceeds the current protection value 600 A. After deduction, the I_{acd} and I_{acq} are replaced with −187.53 and −569.94, respectively. Combination of transfer active balance in RPC, the value of $[I_{\mathrm{acd}}\ I_{\mathrm{acq}}\ I_{\mathrm{bcd}}\ I_{\mathrm{bcq}}]$ is [−187.53 −569.94 187.53 159.8] under the condition of $|I_{\mathrm{ac}}|$being equal to 600 A. The negative sequence current becomes 23.8 A, and all interrelationship constraints are satisfied. But above all, the SQP method is superior to analytical method under any circumstances.

IV. Design and Verification of Self-Adaption Real-Time Optimization

In the previous section, the locomotive load is analyzed at a specific moment under typical working conditions. During actual operation, as the load power and the properties of the locomotive vary from time to time, the load current needs to be obtained promptly, which will be used as the initial variable for optimal control. The self-adaption of the optimization computation is realized by utilizing Symbolic Math Toolbox.

A. Self-Adaption Real-Time Optimization Strategy

For a specific engineering, these parameters of the power grid attribute and devices are preset and the load is the only variable; therefore, self-adaption means timely obtainment of optimal compensation instruction based on variation of loads and voltages. Symbolic reasoning of the MATLAB symbol and millisecond operating rate of the SQP method make possible self-adaption and real-time optimization. The schematic block diagram is shown in Fig. 6.

In the mathematical model, ωL_{a}, ωL_{b}, $U_{\mathrm{max}-}$, $U_{\mathrm{max}+}$, k_{f}, P_{max}, $I_{\mathrm{c\,max}}$, S_{a}, and S_{b} are values used for setup; U_{ad} and U_{bd} are determined by real-time feedback value from feeder; the principle of the real-time solution is as follows.

Step 1: Parameters such as I_{Lad}, I_{Laq} and I_{Lbd}, I_{Lbq} that vary with the working conditions will be detected through load current sensors; U_{ad}, phase a voltage of feeder section, and U_{bd}, phase b voltage of feeder section are detected by voltage transformers.

Step 2: Parameters such as ωL_{a}, ωL_{b}, $U_{\mathrm{max}-}$, $U_{\mathrm{max}+}$, k_{f}, P_{max}, $I_{\mathrm{c\,max}}$, S_{a}, and S_{b} received by the upper computer will be input into the model of optimization problems.

Step 3: A specific expression of an optimization problem will be renewed in every 3 ms via MATLAB Symbolic Math Toolbox in real-time operating state.

Step 4: Write a specific expression (including expressions of objective function and constraint function) of an optimization problem into the corresponding function file, to be called by the SQP algorithm.

Step 5: Give the initial optimizing value according to the principle of active balance of Phase a and Phase b and the load reactive power of each completely compensated. The computational formula is got as follow.

$$\begin{cases} I_{\mathrm{acd}} = (-I_{\mathrm{Lad}} + I_{\mathrm{Lbd}})/2 \\ I_{\mathrm{acq}} = -I_{\mathrm{Laq}} \\ I_{\mathrm{bcd}} = (I_{\mathrm{Lad}} - I_{\mathrm{Lbd}})/2 \\ I_{\mathrm{bcq}} = -I_{\mathrm{Lbd}} \end{cases}. \tag{24}$$

Step 6: The optimal value of I_{acd}, I_{acq}, I_{bcd}, and I_{bcq} is obtained by SQP computation, while satisfying the needs of precision and time, and the minimum module value of the negative sequence current under the current working condition is received too.

Step 7: Results will be displayed on monitor.

B. Application in Project Cases

In this section, the self-adaption real-time optimization strategy will be used under actual working conditions so as to verify

TABLE V
PERFORMANCE COMPARISON BETWEEN ANALYTICAL METHOD AND SQP.

Algorithm	Negative sequence current (A)	Fluctuation voltage (V)	Total power factor	Active power of RPC (MW)	Currents peak of RPC (A)	Transformer winding capacity (MVA)
analytical method	0.0019	$\Delta U_{\mathrm{a}} = -129.3,$ $\Delta U_{\mathrm{a}} = -129.3$	1.0	4.75	$\lvert I_{\mathrm{ac}}\rvert = 296.7$ $\lvert I_{\mathrm{bc}}\rvert = 799.87$	$\sqrt{P_{\mathrm{a}}^2 + Q_{\mathrm{a}}^2} = 9.87$ $\sqrt{P_{\mathrm{b}}^2 + Q_{\mathrm{b}}^2} = 9.87$
SQP method	0.4903	$\Delta U_{\mathrm{a}} = -12.4,$ $\Delta U_{\mathrm{b}} = 530.97$	0.93	2.81	$\lvert I_{\mathrm{ac}}\rvert = 599.96,$ $\lvert I_{\mathrm{bc}}\rvert = 365.47$	$\sqrt{P_{\mathrm{a}}^2 + Q_{\mathrm{a}}^2} = 10.61,$ $\sqrt{P_{\mathrm{b}}^2 + Q_{\mathrm{b}}^2} = 10.57$

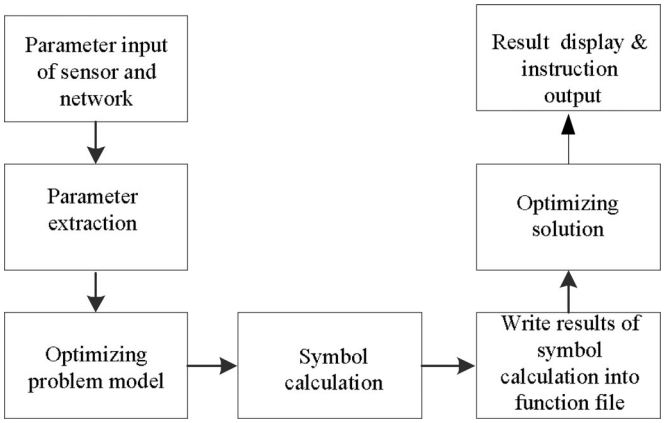

Fig. 6. Design of self-adaption real-time optimization strategy.

the efficacy of the proposed method. Three typical working conditions, namely, traction, braking, and no-load will be selected in every phase load, and nine working conditions will be gained by permutation and combination. Considering the condition that both Phases a and b bear no load is without practical significance and will not be taken into consideration. Therefore, eight working conditions will be discussed, i.e., Phase a traction and Phase b traction, Phase a traction and Phase b braking, Phase a traction and Phase b no-load, Phase a braking and Phase b traction, Phase a braking and Phase b braking, Phase a braking and Phase b no-load, Phase a no-load and Phase b traction, and Phase a no-load and Phase b braking. The parameters of power grid and compensating device are initialized, and values of ωL_{a}, ωL_{b}, $U_{\max -}$, $U_{\max +}$, k_{f}, $P_{\max}$, $I_{\mathrm{c}\max}$, S_{a}, and S_{b}, respectively, are illustrated in Table II. Meanwhile, the measured values of traction network voltages (U_{ad}, U_{bd}) are assumed to be 38 kV. The measured value of load currents such as I_{Lad}, I_{Laq}, I_{Lbd}, and I_{Lbq} are shown in Table VI, and the optimal value of I_{acd}, I_{acq}, I_{bcd}, and I_{bcq} is gained through optimizing under given parameters by using the SQP method, and the optimum negative sequence current values are gained simultaneously. The time consumption are range from 2 to 10 ms, combined with the time delay of optical fiber communication between computer with running SQP and digital controller of RPC, the all time consumption is less than 11 ms, which is faster than the change of locomotive power. So the computational accuracy and time consumption of SQP are both satisfactory.

Among the eight types working conditions mentioned above, state i denotes a condition with both Phases a and b traction, in which the optimum values are –147.7, –581.5, 147.7, and 334.3 A, respectively. It is constrained by the maximum current of RPC at the Phase a port, and the negative sequence current after compensation is 0.4765 A. State ii denotes a condition with Phase a traction and Phase b no-load, in which the optimum values are –357.6, –357.4, 357.6, and 304.4 A, respectively. Each constraint condition is met, and the negative sequence current after compensation is only 0.0133 A. State iii denotes a condition with Phase a traction and Phase b braking, in which the optimum values are –399.9, –200, 399.9, and –100 A, respectively. Each constraint condition is met, and the negative sequence current after compensation is only 0.0144 A. State iv denotes a condition with Phase a no-load and Phase b traction, in which the optimum values are –371.4, 231, 371.4, and –471.2 A, respectively. It is constrained by the maximum current of RPC at the Phase b port, and the negative sequence current after compensation is 7.97133 A. State v denotes a condition with Phase a no-load and Phase b braking, in which the optimum values are –160.8, 183.3, 160.8, and 252.4 A, respectively. Each constraint condition is met, and the negative sequence current after compensation is only 0.0084 A. State vi denotes a condition with Phase a braking and Phase b traction, in which the optimum values are 421.06, –75.5, –421.06, and –354.5 A, respectively. It is constrained by the active power capacity of RPC, and the negative sequence current after compensation is 10.442 A. State vii denotes a condition with Phase a braking and Phase b no-load, in which the optimum values are 117.4, 130.1, –117.4, and –143.1A, respectively. Each constraint condition is met, and the negative sequence current after the compensation is only 0. 0051 A. State viii denotes a condition with Phase a braking and Phase b braking, in which the optimum values are 46.7, 238.5, –46.7, and –450.1 A. Each constraint condition is met, and the negative sequence current after compensation is only 0.0154 A.

To sum up, if each constraint condition is met, satisfactory solution can be gained. Besides, the amplitude of the three-phase current I_{A}, I_{B}, and I_{C} at the HV side is equivalent, and the phases arrange by the direction of positive sequence. It shows that no matter what the working condition is and if all the constraints are satisfied, the optimum value of the negative sequence current can be achieved by optimizing calculation.

TABLE VI
REAL-TIME OPTIMIZATION RESULTS UNDER CHANGING WORKING CONDITIONS

State No.	Values of $I_{\mathrm{Lad}}, I_{\mathrm{Laq}}, I_{\mathrm{Lbd}}, I_{\mathrm{Lbq}}$ (A)	Optimum value (A)	Optimum module value of negative sequence current (A)	Time consumed (s)
State i	$(700, 500, 200, 100)$	$(-147.7, -581.5, 147.7, 334.3)$	0.4765	0.001
State ii	$(800, 200, 0, 0)$	$(-357.6, -357.4, 357.6, 304.4)$	0.0133	0.003
State iii	$(400, 200, -400, 100)$	$(-399.9, -200, 399.9, -100)$	0.0144	0.002
State iv	$(0, 0, -800, 300)$	$(-371.4, 231, 371.4, -471.2)$	7.9713	0.010
State v	$(0, 0, -400, -300)$	$(-160.8, 183.3, 160.8, 252.4)$	0.0084	0.008
State vi	$(-300, -100, 700, 400)$	$(421, -75.5, -421, -354.5)$	10.422	0.010
State vii	$(-300, -100, 0, 0)$	$(117.4, 130.1, -117.4 - 143.1)$	0.0051	0.003
State viii	$(-300, -100, -200, 300)$	$(46.7, 238.5, -46.7, -450.1)$	0.0154	0.003

V. ENGINEERING PROTOTYPE AND EXPERIMENTAL ANALYSIS

A. Prototype System Parameters

In order to validate the theoretical analysis above, the demonstration project was built as shown in Fig. 7. Power circuit and variable definition of traction supply system are consistent with Fig. 1 and Table II. RPC is composed by four single-phase multiwinding transformer and eight independent back-to-back converters. Each inverter cabinet mainly comprises a back-to-back 1MVA module, a 100-Hz resonance branch, and a control unit, as shown in Fig. 7(a). Eight inverter cabinets, a water cooling system, and the master controller cabinets are installed in a container, as shown in Fig. 7(b). Four single-phase multiple windings transformers with the one receiving 27.5-kV voltage and the remaining four exporting 970 V, and connecting reactors are installed in outdoor as shown in Fig. 7(c). Power scheduling strategy based on SQP and processing vectors monitoring are the main function of the master controller, and each control unit controls the corresponding inverter by referential power. Load current $\dot{I}_{\mathrm{La}}$ and $\dot{I}_{\mathrm{Lb}}$ are measured by detecting feeder currents, and $\dot{I}_{\mathrm{a}}$ and $\dot{I}_{\mathrm{b}}$ are measured by detecting busbar bridge currents. For the sake of contrastive analysis, it assumes that $\dot{I}_{\mathrm{La}}$, $\dot{I}_{\mathrm{Lb}}$ and $\dot{I}_{\mathrm{a}}$, $\dot{I}_{\mathrm{b}}$ are the low-voltage winding currents of traction transformer before and after compensation.

B. RPC Control Strategy

RPC is the actuator, and these optimal values of active and reactive currents based on SQP method are implemented by RPC. Each dc generatrix is mutual independence, so every ac–dc–ac converter can be independently controlled. Double closed-loop control with direct active current control and dc voltage regulation control are adopted separately, as indicated in Fig. 8. The former can be shown with Fig. 8(a), it is composed of the following processing blocks:

1) Current close loop: The optimal value I_{acd} and I_{acq} are divided into eight equal parts, and as reference of Proportional-Integral (PI) controller. $I_{\mathrm{acd\text{-}k}}$ and $I_{\mathrm{acq\text{-}k}}$ are the output values of ac–dc converter in the side of Phase a, and they are feedback quantities of PI controller.
2) Decoupling control: The independent control of the two supply current components are realized by the

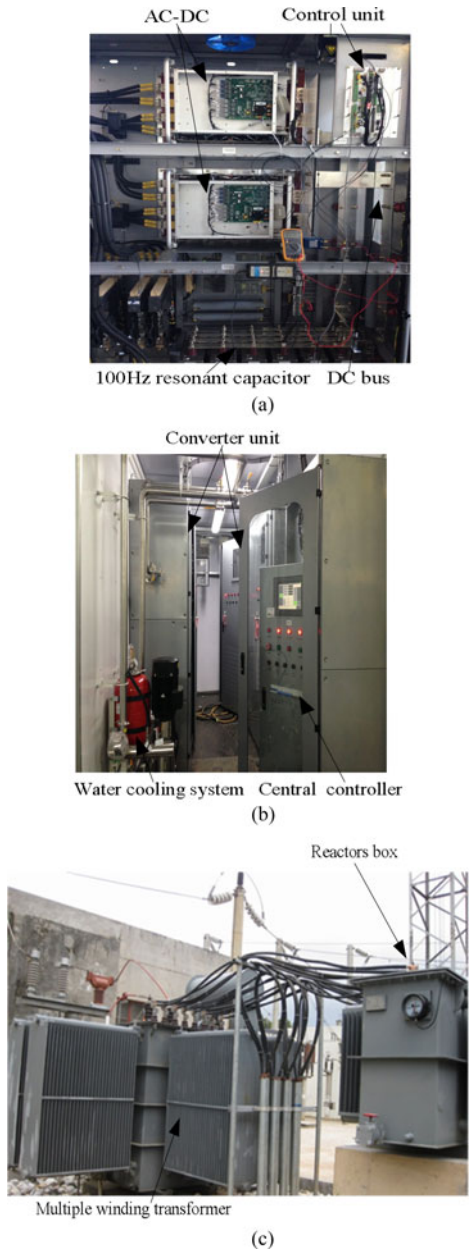

Fig. 7. Photos of RPC equipment. (a) Single back-to-back converter. (b) Indoor part of RPC. (c) One of multiple transformer and reactors.

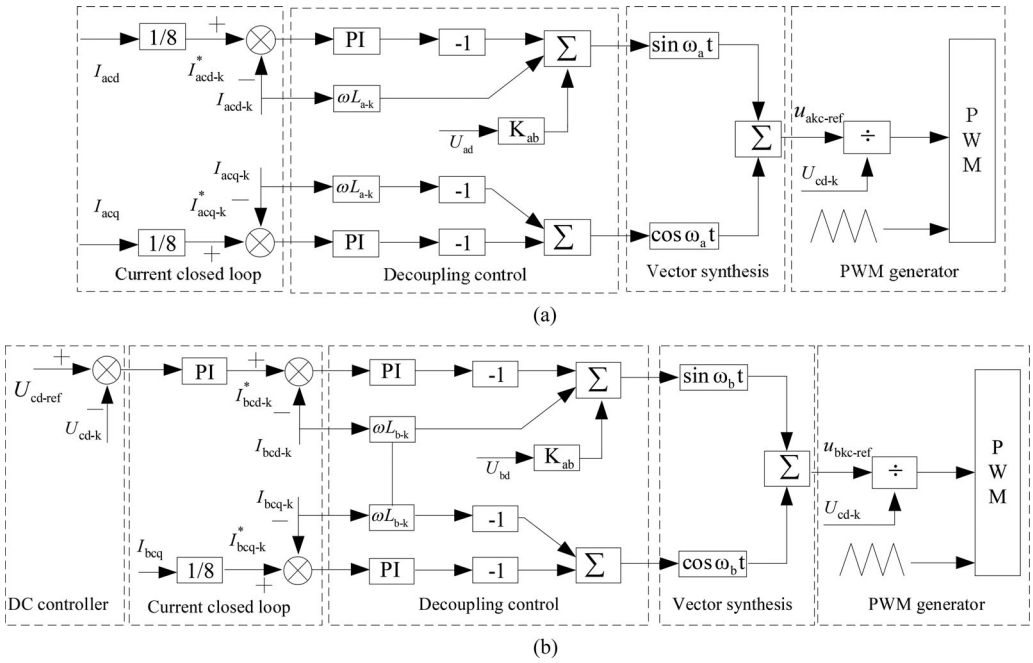

Fig. 8. Control block diagram of RPC. (a) RPC control with active current direct control. (b) RPC control with dc voltage regulation control.

traditionally decoupled control based on link reactance $\omega L_{\text{a-k}}$. The variable K_{ab} is the ratio from 27.5 kV to 970 V.

3) Vector synthesis: $\sin\omega_{\text{a}}\text{t}$ and $\cos\omega_{\text{a}}\text{t}$ are gained by PLL with the voltage of Phase a, and the total vector $u_{\text{akcq-ref}}$ can calculated by trigonometric calculation.
4) PWM generator: Per unit value of modulated wave is obtained by the ratio between $u_{\text{akcq-ref}}$ and dc voltage $U_{\text{cd-k}}$, and the PWM pulses are generated through modulated wave compared with triangular wave.

DC voltage regulation control as shown in Fig. 8(b). Compared with Fig. 8(a), reference of active current is adjusted by dc voltage control based on PI rather than the result of optimization calculation, but the reference of reactive power current is provided by SQP method.

C. Effectiveness Analysis

The voltage and currents waveforms in Fig. 9 corresponds to the State i in Table VI, four channel waveforms in Fig. 9(a) are $\dot{U}_{\text{A}}$, $\dot{I}_{\text{La}}$, $\dot{I}_{\text{Lb}}$, and $\dot{I}_{\text{a}}$, respectively, and four channel waveforms in Fig. 9(b) are $\dot{U}_{\text{A}}$, $\dot{I}_{\text{La}}$, $\dot{I}_{\text{a}}$, and $\dot{I}_{\text{b}}$, respectively. The transformation ratio of voltage channel is from 63.5 kV to 10 V, and the transformation ratio of current is 1000 to 5 A. By comparison, the phase angle of $\dot{I}_{\text{La}}$ and $\dot{I}_{\text{Lb}}$ are –65.5° and –116.5°, respectively, $\dot{I}_{\text{a}}$ is the same vector with $\dot{I}_{\text{La}}$, and $\dot{I}_{\text{b}}$ is the same vector with $\dot{I}_{\text{Lb}}$ before compensation. The phase angle form $\dot{I}_{\text{a}}$ to $\dot{I}_{\text{b}}$ is 51°, and their root mean square (RMS) are 3.02 A and 0.79 A, respectively, and the distribution of currents is asymmetric. After the compensation for RPC based on SQP, the phase angle of $\dot{I}_{\text{a}}$ and $\dot{I}_{\text{b}}$ turn into –21.6° and –141.3°, and their RMS

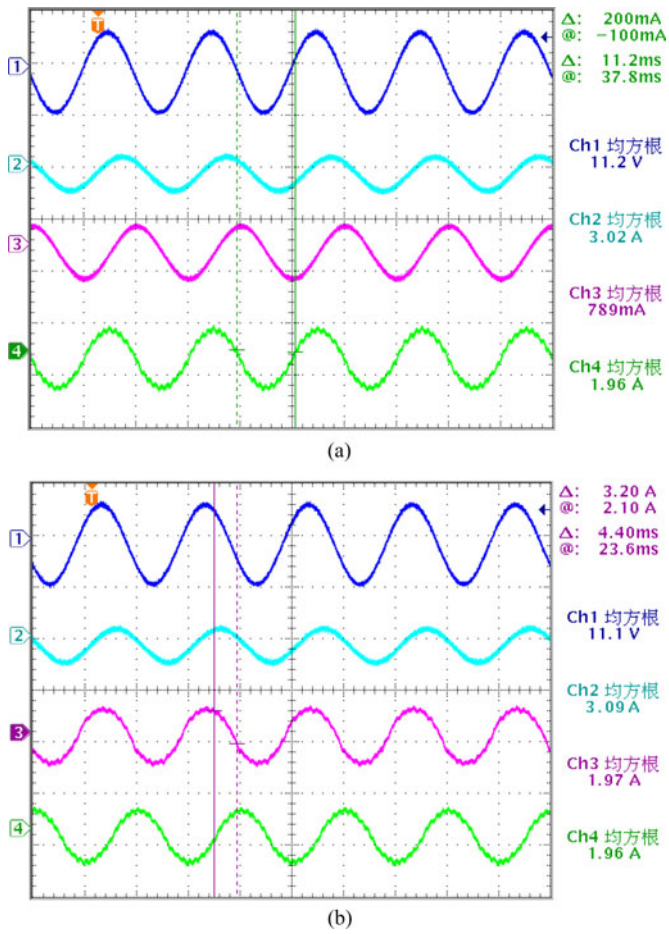

Fig. 9. *V–I* waveforms in State i. (a) Voltage and current waveforms of loads. (b) Voltage and current waveforms of RPC.

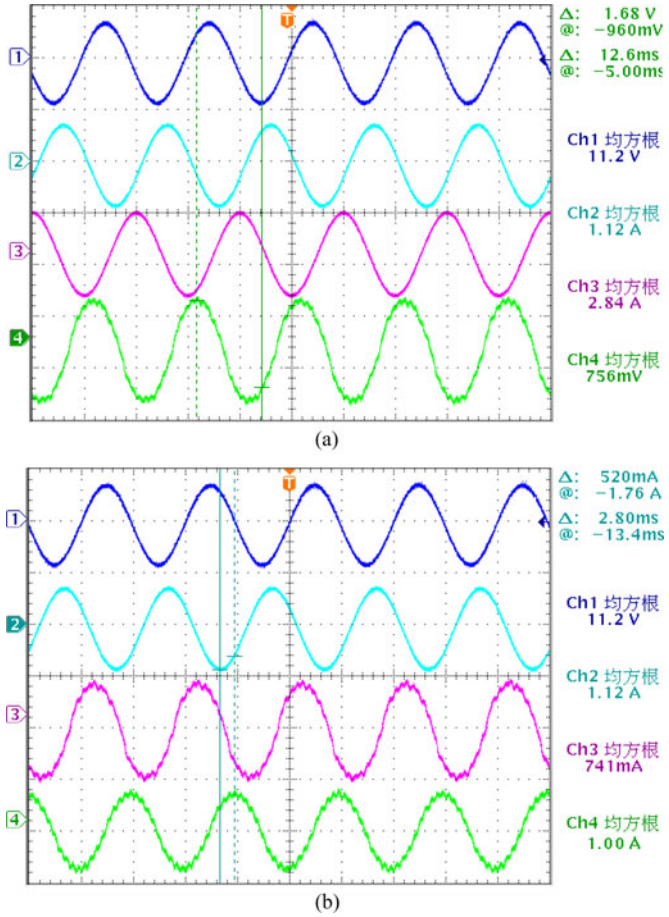

Fig. 10. *V–I* waveforms in State vi. (a) Voltage and current waveforms of loads. (b) Voltage and current waveforms of RPC.

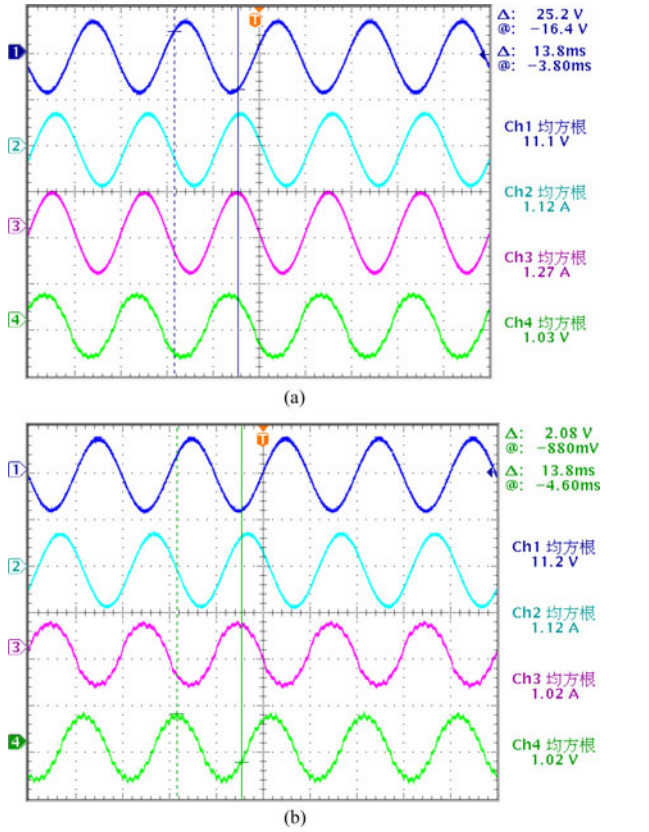

Fig. 11. *V–I* waveforms in State viii. (a) Voltage and current waveforms of loads. (b) Voltage and current waveforms of RPC.

change into 1.97 A and 1.96 A, respectively. The current after compensation basically meet the condition of positive sequence distribution.

The variable and channel definition in Fig. 10 is same with Fig. 9 corresponds to the State vi in Table VI. By comparison, the phase angle of $\dot{I}_a$ and $\dot{I}_b$ before compensation are –228.4° and –119.7°, and their RMS are 1.12 and 2.84 A, respectively, and the distribution of currents is asymmetric in character. After the compensation for RPC based on SQP, the phase angle of $\dot{I}_a$ and $\dot{I}_b$ turn into 25.5° and –99.3°, and their RMS change into 0.75 and 1.0 A, respectively. The current after compensation is near to meet the need of positive sequence distribution.

The variable and channel definition in Fig. 11 is same with Fig. 9 corresponds to the State viii in Table VI. On the same principle, the phase angle of $\dot{I}_a$ and $\dot{I}_b$ before compensation are –228.4° and –213.7°, and their RMS are 1.12 and 1.27 A, respectively, and the distribution of currents is asymmetric. After the compensation for RPC based on SQP, the phase angle of $\dot{I}_a$ and $\dot{I}_b$ turn into 180° and 58.68°, and their RMS is identical and equal to1.02 A. The current after compensation is near to meet the need of positive sequence distribution.

Experimental results from above are consistent with theoretical inference, and the mathematical model with minimum negative sequence current and SQP method are further verified.

VI. Conclusion

In this paper, the V/v traction power supply system with RPC is used as the object of study to analyze the generation and compensation mechanisms of negative sequence current. On this basis, a mathematical model for minimum module value of the negative sequence current is proposed under the premise that constraints such as power factor, voltage fluctuation, and capacity are met. To solve the multidimensional multi restrained nonlinear optimization problem, the SQP method and the MIP method are comparatively analyzed. The results show that the former is more efficient and more suitable for solving the small-scale optimization problems. Finally, the self-adaption real-time solution method is established based on MATLAB, by which the optimum control variable of RPC can be obtained as per real time working condition of the locomotive load, and a detailed analysis has been carried out under eight typical working conditions by simulation and experiment. Therefore, it is concluded that this algorithm is able to realize optimizing solutions under any working conditions and when all the constraints are taken into account. The feasibility and veracity of this mathematical model and algorithm are verified.

REFERENCES

[1] S. F. Fan, J. Xiong, K. Zhang, L. Q. He, and W. C. Zhao, "Decoupling control scheme of high power four-quadrant converters for traction," in *Proc. Chin. Soc. Electr. Eng.*, vol. 19, no. 21, pp. 63–70, Jul. 2012.

[2] Q. Z. Li, "On some key technical problems in the development of traction power supply system for high-speed railway in china," *J. China Railway Soc*., vol. 32, no. 4, pp. 119–124, Aug. 2010.

[3] H. Q. Wang, Y. J. Tian, and Q. C. Gui, "Evaluation of negative-sequence current injecting into the public grid from different traction substation in electrical railways," in *Proc. 20th Int. Conf. Exhib. Elect. Distrib.*, ution, Prague, Czech Republic, Jun. 2009, pp 1–4.

[4] P. E. Sutherland, M. Waclawiak, and M. F. McGranaghan, " System impacts evaluation of a single-phase traction load on a 115-kv transmission system," *IEEE Trans. Power Del.*, vol. 21, no. 2, pp. 837–844, Apr. 2006.

[5] Z. W. Zhang, B. Wu, J. S. Kang, and L. F. Luo, "A multi-purpose balanced transformer for railway traction applications," *IEEE Trans. Power Del.*, vol. 24, no. 2, pp. 711–718, Apr. 2009.

[6] A. Zupan, A. T. Teklic, and B. Filipovic-Grcic, "Hyperlink modeling of 25 kv electric railway system for power quality studies," in *Proc. IEEE EUROCON*, Zagreb, Jul. 2013, pp. 844–849.

[7] I. G. Sirbu, P. M. Nicolae, and R. Bojoi, "Solution for the power quality improvement in a transportation system," in Proc. 14th Int. Power Electron. Motion Control Conf., Ohrid, Sep. 2010, pp. 32–37.

[8] S. F. Xie, and Q. Z. Li, "Study on impact of high speed train regenerative braking on negative sequence," *J. China Railway Soc.*, vol. 33, no. 7, pp. 14–18, Jul. 2011.

[9] P. C. Tan, P. C. Loh, and D. G. Holmes, " Optimal Impedance termination of 25-kv electrified railway systems for improved power quality," *IEEE Trans. Power Del.*, vol. 20, no. 2, pp. 1703–1710, Apr. 2005.

[10] P. Chaudhary, S. Samanta, and P. Sensarma, "Input-series-output- parallel connected buck-rectifier for high-voltage applications," *IEEE Trans. Ind. Electron.*, vol. 20, no. 99, pp. 1–9, Jun. 2014.

[11] X. He, Z. Shu, X. Peng, Q. Zhou, Y. Zhou, Q. Zhou, and S. Gao, "Advanced in-phase traction power supply system based on three-phase to single-phase converter," *IEEE Trans. Power Electron.*, vol. 29, no. 10, pp. 5323–5333, Nov. 2014.

[12] S. Zhuo, J. Xinjian, Z. Dongqi, and Z. Guixin, "A novel active power quality compensator topology for electrified railway," *IEEE Trans. Ind. Electron.*, vol. 19, no. 4, pp. 1036–1042, Jul. 2004.

[13] T. Pee-Chin, L. P. Chiang, and D. G. Holmes, "A Robust multilevel hybrid compensation system for 25-kv electrified railway applications," *IEEE Trans. Ind. Electron.*, vol. 19, no. 4, pp. 1043–1052, Jun. 2004.

[14] Z. Sun, X. J. Jiang, D. Q. Zhu, and G. X. Zhang, "A novel active power quality compensator topology for electrified railway," *IEEE Trans. Ind. Electron.*, vol. 19, no. 4, pp. 1036–1042, Jul. 2004.

[15] J. J. Wang, C. Fu, and Y. Zhang, "SVC control system based on instantaneous reactive power theory and fuzzy pid," *IEEE Trans. Ind. Electron.*, vol. 55, no. 4, pp. 1658–1665, Apr. 2008.

[16] Y. Mochinaga, M. Takeda, and K. Hasuike, "Static power conditioner using GTO converters for ac electric railway," in *Proc. Power Convers. Conf.*, Yokohama, Japan, Apr. 2002, pp. 641–646.

[17] A. Luo, C. P. Wu, and J. Shen, "Railway static power conditioners for high speed train traction power supply systems using three phase v/v transformers," *IEEE Trans. Power Electron.*, vol. 26, no. 10, pp. 2844–2586, Mar. 2011.

[18] C. P. Wu, A. Luo, J. Shen, F. J. Ma, and S. J. Peng, "A negative sequence compensation method based on a two-phase three-wire converter for a high-speed railway traction power supply system," *IEEE Trans. Power Electron*., vol. 27, no. 2, pp. 706–717, Jun. 2012.

[19] A. Luo, F. J. Ma, C. P. Wu, S. Q. Ding, Q. C. Zhong, and Z. K. Shuai, "A dual-loop control strategy of railway static power regulator under v/v electric traction system," *IEEE Trans. Power Electron.*, vol. 26, no. 7, pp. 2079–2091, Jul. 2011.

[20] F. J. Ma, A. Luo, X. Y. Xu, H. G. Xiao, C. P. Wu, and W. Wang, "A simplified power conditioner based on half-bridge converter for high-speed railway system," *IEEE Trans. Ind. Electron.*, vol. 60, no. 2, pp. 728–738, Feb. 2013.

[21] Z. L. Shu, S. F. Xie, and Q. Z. Li, "Single phase back to back converter for active power balancing, reactive power compensation and harmonic filtering in traction power system," *IEEE Trans. Power Electron.*, vol. 26, no. 2, pp. 334–343, Feb. 2011.

[22] Z. L. Shu, S. F. Xie, K. Lu, Y. Z. Zhao, X. Q. Nan, D. Q. Qiu, F. L. Zhou, S. B. Gao, and Q. Z. Li, "Digital detection, control, and distribution system for co-phase traction power supply application," *IEEE Trans. Ind. Electron.*, vol. 60, no. 5, pp. 1831–1839, May 2013.

[23] K.W. Lao, N. Dai, W.G. Liu, and M.C. Wong, "Hybrid Power quality compensator with minimum dc operation voltage design for high-speed traction power systems," *IEEE Trans. Power Electron.*, vol. 28, no. 4, pp. 2024–2036, Apr. 2013.

[24] J. L. Hu, Z. P Wu, H. McCann, L. E. Davis, and C. G. Xie, "Sequential quadratic programming method for solution of electromagnetic inverse problems," *IEEE Trans. Antennas Propag.*, vol. 53, no. 8, pp. 2680–2687, Aug. 2005.

[25] H. Wei, H. Sasaki, and R. Yokoyama, "An application of interior point quadratic programming algorithm to power system optimization problems," *IEEE Trans. Power Syst.*, vol. 11, no. 1, pp. 260–266, Feb. 1996.

Dinghua Zhang was born in Shuangfeng of Hunan, China in 1979. He received the M.Sc. and Ph.D. degrees in control science and engineering from Central South University, Changsha, China, in 2006 and 2011, respectively.

In 2006, he joined CSR Zhuzhou Electric Locomotive Research Institute Co., Ltd., where he was a Engineer from 2008 to 2011, and is currently a Senior Engineer and a project manager in CSR Research of Electrical Technology & Material Engineering. His research interests include traction power system, power quality, cascade multilevel converter, and control in power system.

Zhixue Zhang was born in Longhui of Hunan, China in 1973. He received the M.Sc. degree in electrical engineering from Hunan University, Changsha, China, in 2002, and the Ph.D. degree from Zhejiang University, Hangzhou, China, in 2005.

In 2005, he joined CSR Zhuzhou Electric Locomotive Research Institute Co. Ltd., where he was a Senior Engineer from 2008 to 2012, and is currently a professorate senior engineer in CSR Research of Electrical Technology & Material Engineering. His research interests include locomotive control and pulse width modulation rectifier.

Weian Wang was born in Shuangfeng of Hunan, China in 1975. He received the M.Sc. and Ph.D. degrees in control science and engineering from Central South University, Changsha, China, in 2005 and 2013, respectively.

In 1996, he joined CSR Zhuzhou Electric Locomotive Research Institute Co. Ltd, where he was a Senior Engineer from 2006 to 2011, and is currently a Professorate Senior Engineer in Zhuzhou CSR Times Electric Co. Ltd . His research interests include reactive power compensator, active power filter, and control technology.

Yanling Yang was born in Zhuzhou of Hunan, China in 1994. She is currently a student of Beijing Institute of Technology, Electronic Science and technology.

In 2014, she became a trainee in CSR Zhuzhou Electric Locomotive Research Institute Co., Ltd., Her research interest is signal processing to power electronic converters.